after reaction. This conclusion was substantiated by the X-ray diffraction results which did not indicate any differences between a fresh and a used catalyst.

Summarizing the results, it appears that the different selectivities observed for different samples can be correlated with the different crystallite sizes. The dependence becomes important for sizes smaller than about 10 nm. Evidence does suggest that the effect is not due to the formation of other detectable iron oxide phases or compounds due to reaction, nor to the pore diffusional effect. In addition, the silica support stabilizes the iron oxide crystallites against sintering.

What are the likely causes of the crystallite size dependence of selectivity? A definite answer is not provided by this study. There are a number of possibilities. First, the reaction may be crystal face specific. Thus, when the ratios of different crystal faces change with crystallite size, the selectivity changes accordingly. Detailed knowledge of the distribution of exposed crystal faces is not available. X-ray diffraction data showed that the relative intensities of the various diffraction peaks were similar for the different catalysts. This implied that the shape of the α-Fe$_2$O$_3$ crystallites remained the same for the different sizes and that epitaxial growth of α-Fe$_2$O$_3$, which might lead to the exposure of one particular crystal plane, was not present. Second, the production of butadiene may require a specific site such as anion or cation vacancies. The density of such specific sites may be higher on smaller crystallites. Indeed, the requirement of a site involving an anion vacancy has been proposed for butadiene production.[6] Third, the reaction mechanism has been proposed to involve an oxidation–reduction cycle of the catalyst.[6-11] Therefore, if the oxidation–reduction property of the oxide crystallite depends on its size, its catalytic propety would also change. This has been used to explain the effect of a second

component in ferrites.[11] The dependence of the oxidation–reduction property on crystallite size for unsupported oxides is not well-known. In silica-supported samples, it has been reported that small iron oxide crystallites are much more difficult to be reduced than large crystallites.[12-16] This may be a result of the silica–oxide interaction coupled with the crystallite size effect. Fourth, it was reported that the difference between the selectivities for butadiene on α- and γ-Fe$_2$O$_3$ is partly due to the different rates of desorption of the butadiene product and partly due to the different susceptibility of the butadiene or its precursor to degradation by weakly adsorbed oxygen.[17,18] Therefore, it is conceivable that the activation of this weakly adsorbed oxygen on α-Fe$_2$O$_3$ is crystallite size dependent. This would be possible if activation of such oxygen requires charge transfer from the solid. Such activation could be more difficult on smaller crystallites for which electron transfer results in a large shift in the potential of the entire crystallite, thereby making such electron transfer more difficult. This results in a slower rate of degradation of adsorbed butadiene and a higher selectivity.

In conclusion, it is demonstrated that the selectivity for butadiene production in the oxidation of butene on α-Fe$_2$O$_3$ depends on the crystallite size of iron oxide. This phenomenon may be due to changes in a number of properties of the oxide crystallites. In contrast, the specific activity in butene conversion does not depend on crystallite size. The beneficial effect of the silica gel support in stabilizing iron oxide against sintering is also demonstrated.

(6) F. E. Massoth and D. A. Scarpiello. *J. Catal.*, **21**, 294 (1971).
(7) M. C. Kung, W. H. Cheng, and H. H. Kung, *J. Phys. Chem.*, **83**, 1737 (1979).
(8) R. Rennard and W. Kehl, *J. Catal.*, **21**, 282 (1971).
(9) M. Gibson and J. Hightower, *J. Catal.*, **41**, 420 (1976).
(10) W. R. Cares and J. Hightower, *J. Catal.*, **23**, 193 (1971).
(11) H. H. Kung, B. Kundalkar, M. C. Kung, and W. H. Cheng, *J. Phys. Chem.*, **84**, 382 (1980).

(12) G. B. Raupp and W. N. Delgass, *J. Catal.*, **58**, 337 (1979).
(13) M. C. Hobson and H. M. Gager, *J. Catal.*, **16**, 254 (1970).
(14) N. Malathi and S. P. Puri, *J. Phys. Soc. Jpn.*, **31**, 1418 (1971).
(15) J. A. Amelse, J. B. Butt, and L. H. Schwartz, *J. Phys. Chem.*, **82**, 558 (1978).
(16) E. Unmuth, L. H. Schwartz, and J. B. Butt, *J. Catal.*, **61**, 242 (1980).
(17) B. Yang and H. H. Kung, *J. Catal.*, **77**, 410 (1982).
(18) B. Yang, M. C. Kung, and H. H. Kung, submitted for publication in *J. Catal.*

Reaction of Hydrogen Atom with Benzene: Kinetics and Mechanism

J. M. Nicovich and A. R. Ravishankara*

Molecular Sciences Branch, Engineering Experiment Station, Georgia Institute of Technology, Atlanta, Georgia 30332 (Received: July 14, 1983)

The rate coefficients for the reactions H + C$_6$H$_6$ → products (k_1) (1), H + C$_6$D$_6$ → products (k_2) (2), D + C$_6$H$_6$ → products (k_3) (3), and D + C$_6$D$_6$ → products (k_4) (4) have been measured in the temperature range of 298–1000 K by using the pulsed photolysis–resonance fluorescence technique. On the basis of the obtained kinetic information, it is shown that the primary path in all these reactions is addition of the atom to the benzene ring to form cyclohexadienyl radical. The rate coefficient for the thermal decomposition of the cyclohexadienyl radical has also been measured. When the rate coefficients for the formation and the decomposition of the cyclohexadienyl radical are used, the standard heat of formation of cyclohexadienyl radical at 298 K is calculated to be 45.7 kcal/mol. The measured values of k_1–k_4 are compared with the results of previous investigations. Most of the observed kinetic behavior in these reactions has been explained on the basis of the addition–decomposition reaction scheme.

Introduction

Reactions of simple free radicals such as OH, O(^{3}P), and H(^{2}S) with aromatic hydrocarbons play important roles in the initiation and propagation of aromatic hydrocarbon combustion. The reactions of H(^{2}S) could play a major role in the hydrogenation of aromatics as well. Direct studies of these free-radical reactions with aromatic hydrocarbons have been limited even though the reactions involving nonaromatic hydrocarbons have been exten-

sively investigated. In recent years we have initiated systematic studies of radical–aromatic hydrocarbon reactions with the aim of measuring kinetic parameters and elucidating the reaction mechanisms as a function of temperature (up to ~1200 K) using the pulsed photolysis–resonance fluorescence technique.[1-4] The

(1) F. P. Tully, A. R. Ravishankara, R. L. Thompson, J. M. Nicovich, R. C. Shah, N. M. Kreutter, and P. H. Wine, *J. Phys. Chem.*, **85**, 2262 (1981).

previous studies have dealt with the reactions of OH and O(^{3}P). The present paper is the first in a series which describes our studies of H(^{2}S) atom reactions with aromatic hydrocarbons and is concerned with reaction of H(^{2}S) with benzene:

$$H(^2S) + C_6H_6 \xrightarrow{k_1} \text{products} \qquad (1)$$
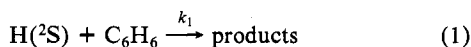
Yang[5] measured k_1 relative to the reaction of H with propane using γ-radiolysis and estimated the activation energy for reaction 1 to be 3.9 kcal/mol. The extrapolation of his results to 298 K yields k_1(298 K) = 1.65×10^{-14} cm^3 molecule^{-1} s^{-1}. Sauer and co-workers[6,7] studied this reaction using the pulse radiolysis technique by following the UV absorption of a transient (cyclohexadienyl radical) formed in reaction 1. Sauer and Ward[6] measured k_1 to be 6.1×10^{-14} cm^3 molecule^{-1} s^{-1} at 298 K and estimated the activation energy to be 3.3 kcal/mol based on a few measurements over a very limited temperature range. This activation energy was later revised upward to 4.3 kcal/mol by Sauer and Mani.[7] Kim et al.[8] studied reaction 1 using a discharge flow tube equipped with either an ESR or a mass spectrometer detection system. They observed isotopic exchange in the reaction of D(^{2}S) with C$_6$H$_6$ and had to use stoichiometric correction factors to estimate their atom concentrations. They recommended the following Arrhenius expression based on their measurements:

$$k_1 = (1.00 \pm 0.16) \times$$
$$10^{-11} \exp\{(-2700 \pm 200)/RT\} \text{ cm}^3 \text{ molecule}^{-1} \text{ s}^{-1}$$

Knutti and Buhler[9] used a discharge flow tube equipped with a mass-spectrometric sampling detector and measured k_1 to be $(3.0 \pm 0.3) \times 10^{-14}$ cm^3 molecule^{-1} s^{-1} at 298 K. Hoyermann et al.[10] used a discharge flow apparatus equipped with an ESR detector for H atom and a mass spectrometer for hydrocarbon concentration measurements and studied reaction 1 between 296 and 493 K. They reported the following expression to describe their results:

$$k_1 = 1.15 \times$$
$$10^{-11} \exp[-\{1.87 \pm 0.35) \times 10^3/T\} \text{ cm}^3 \text{ molecule}^{-1} \text{ cm}^{-3}$$

The above description clearly shows the disparity in the values of k_1 measured till now.

Benson and Shaw,[11] in the course of their investigation of the pyrolysis of 1,3-cyclohexadiene, proposed that the initial step in reaction 1 is the addition of H atoms to the benzene ring to form cyclohexadienyl radicals. This finding was evoked to explain the deuterium exchange seen by Kim et al.[8] as well as Knutti and Buhler.[9] Bennett and Mile[12] have shown cyclohexadienyl to be the product of reaction 1 at 77 K, using the matrix isolation–ESR technique. In addition, the UV absorption spectrum seen upon the reaction of H with benzene has been ascribed to the cyclohexadienyl radical.[7]

Both Kim et al.[8] and Knutti and Buhler[9] carried out a competitive experiment where C$_6$H$_6$ and C$_6$D$_6$ were reacting with the same pool of H atoms to find the ratio of rate coefficients k_1/k_2.

$$H + C_6D_6 \xrightarrow{k_2} \text{products} \qquad (2)$$
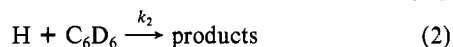
Assuming reactions 1 and 2 to be the rate-determining steps for the depletion of C$_6$H$_6$ and C$_6$D$_6$ in excess H atoms, Kim et al. deduced k_1/k_2 = 0.44 while Knutti and Buhler obtained 0.53
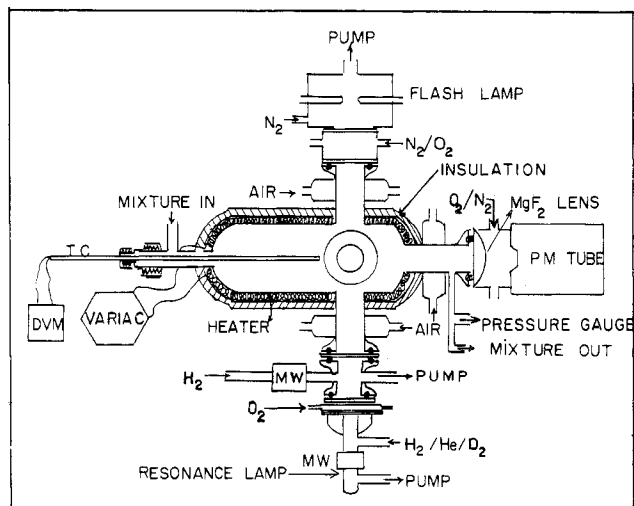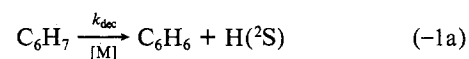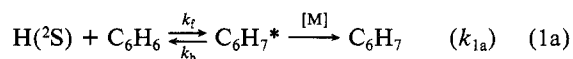

Figure 1. Schematic diagram of the flash photolysis–resonance fluorescence apparatus used in the present study. For ease of depiction, the flash lamp is shown opposite to the resonance lamp. In the actual setup they were at right angles to each other.

for the same ratio. This observation was interpreted to show the absence of ring hydrogen abstraction by H atoms. One other piece of mechanistic information comes from the work of Sauer and Mani, who studied the reactions of H atoms with a series of substituted benzenes. They could correlate the observed reactivity with the Hammett functions for the substituents. Sauer and Mani, therefore, concluded that H atoms react with aromatic hydrocarbons via electrophillic addition.

In this paper, we describe our studies of reaction 1 over the temperature range 298–1000 K. The experiments were carried out by using the flash photolysis–resonance fluorescence technique adapted for H atom studies. To avoid confusion later on in the paper, we would like to present, "up front", the possible reactions that can take place in this system. These reactions are

$$H(^2S) + C_6H_6 \underset{k_b}{\overset{k_f}{\rightleftharpoons}} C_6H_7^* \xrightarrow{[M]} C_6H_7 \qquad (k_{1a}) \quad (1a)$$

$$C_6H_7 \xrightarrow[{[M]}]{k_{dec}} C_6H_6 + H(^2S) \qquad (-1a)$$

$$H(^2S) + C_6H_6 \xrightarrow{k_{1b}} C_6H_5 + H_2 \qquad (1b)$$

Detailed kinetic evidence will be presented to show the importance of the addition–decomposition pathway reactions 1a and −1a and the negligible importance of reaction 1b. To unravel various features of the above scheme, the following two reactions were studied in addition to reactions 1 and 2:

$$D + C_6H_6 \xrightarrow{k_3} \text{products} \qquad (3)$$

$$D + C_6D_6 \xrightarrow{k_4} \text{products} \qquad (4)$$
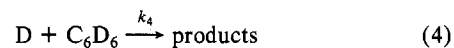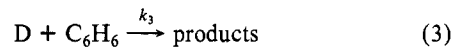
Experimental Methods and Results

In the course of the investigations reported here, experiments aimed at measuring the rate coefficients k_1–k_4, the yield of products (at one temperature), and the rate of decomposition of the reaction product back to reactants were carried out. All these measurements were made by using the well-established technique of flash photolysis–resonance fluorescence which has been described in the literature. However, there were certain subtle differences in the application of the technique which will be described in this section.

A schematic diagram of the apparatus in the configuration employed in the present study is shown in Figure 1. Many of the details such as (1) the construction, the heating, and the temperature measurements in the cell, (2) the configuration of the resonance lamp, flash lamp, and the PM tube, (3) the detailed procedure for the introduction of stable species to the reactor and

(2) J. M. Nicovich, R. L. Thompson, and A. R. Ravishankara, *J. Phys. Chem.*, **85**, 2913 (1981).

(3) J. M. Nicovich, C. A. Gump, and A. R. Ravishankara, *J. Phys. Chem.*, **86**, 1684 (1982).

(4) J. M. Nicovich, C. A. Gump, and A. R. Ravishankara, *J. Phys. Chem.*, **86**, 1690 (1982).

(5) K. Yang, *J. Am. Chem. Soc.*, **84**, 3795 (1962).

(6) M. C. Sauer, Jr., and B. Ward, *J. Phys. Chem.*, **71**, 3971 (1967).

(7) M. C. Sauer, Jr., and I. Mani, *J. Phys. Chem.*, **74**, 59 (1970).

(8) P. Kim, J. H. Lee, R. J. Bonanno, and R. B. Timmons, *J. Chem. Phys.*, **59**, 4593 (1973).

(9) R. Knutti and R. E. Buhler, *Chem. Phys.*, **7**, 229 (1975).

(10) K. Hoyermann, A. W. Preus, and H. Gg. Wagner, *Ber. Bunsenges. Phys. Chem.*, **79**, 156 (1975).

(11) S. W. Benson and R. Shaw, *J. Am. Chem. Soc.*, **89**, 5351 (1967).

(12) J. E. Bennett and B. Mile, *J. Chem. Soc., Faraday Trans. 2*, **69**, 1398 (1973).

the determinations of their concentrations in the reactor, and (4) the measurement of the concentration of benzenes in stock mixtures have been described in a previous paper dealing with $O(^3P)$ reaction with benzene and toluene.[3] Since the same procedures were used in the present study, they will not be repeated. Only a few important aspects will be pointed out in the next paragraph.

The temperature of the gases flowing through the reactor under pressure conditions identical with those in the experiment was measured with a thermocouple at the reaction zone (the volume produced by the intersection of the photolysis and the resonance radiation beams). The accuracy of the temperature measurement has been estimated to be ± 12 K at 1000 K and ± 2 K at 500 K.[3] In most experiments, the output of the flash lamp was filtered by a quartz widow. However, in some experiments various amounts of O_2 were introduced between the flash lamp and the reactor to eliminate light with $\lambda < 185$ nm. The Lyman-α (H atom resonance) radiation was generated by subjecting high-purity helium to a microwave discharge. The output of the resonance lamp was filtered by 760 torr cm of O_2 to remove oxygen resonance radiation as a well as nitrogen lines around 140 nm. In addition, the fluorescence was filtered by 1000 torr cm of O_2 before being detected by the PM tube. In experiments where D atoms were monitored, a small amount of D_2 was added to the He flowing through the resonance lamp. Since it is impossible to completely remove hydrogen-containing species from He, the lamp always puts out Lyman-α radiation. This line was filtered by H atoms flowing in a filter cell which was placed between the resonance lamp and the reactor. Under these conditions H atoms could not be detcted, as shown by the lack of a signal upon generating H atoms in the reactor. When H atoms were to be detected, D_2 flow into the lamp was cut off and the microwave discharge producing H atoms in the filter cell was turned off. Under these conditions, D atoms were not detected as shown, again, by the lack of a signal when D atoms were generated in the reactor. By this method, H atoms and D atoms could be detected with complete specificity.

The stock gases used in this study were obtained from Matheson Gas Products and had the following stated purities: Ar > 99.9995%, O_2 > 99.98%. These gases were used as supplied. Benzene was purchased from J. T. Baker Co. and had an analyzed purity of >99.99%. The deuterated benzene was obtained from Merck Sharpe and Dohme, Canada, Ltd. Its chemical purity was >99.99% and the isotopic purity was >99.99% D. Both these liquids were degassed before use. D_2O was obtained from Bio-Rad Laboratories. Its isotopic purity was 99.99% D. Both D_2O and double-distilled H_2O were degassed several times before use.

Kinetics Studies. The measurements of k_1-k_4 were carried out under pseudo-first-order conditions with the concentrations of the atoms kept much lower than those of C_6H_6 and C_6D_6. H atoms were produced by the photolysis of C_6H_6 or H_2O while D atoms were similarly produced by using the deuterated analogues. The concentrations of H (or D) atoms ranged from 1×10^{10} to 5×10^{11} cm^{-3} in all of the kinetics experiments. (The detection sensitivity of our apparatus was estimated by photolyzing a known concentration of HCl at 193 nm with an ArF laser.) The concentration of C_6H_6 and C_6D_6 ranged from 1×10^{14} to 5×10^{15} cm^{-3}. The Ar bath gas pressure ranged from 10 to 200 torr, with most experiments being carried out at 100 torr. Under these concentration conditions, the temporal profile of $H(^2S)$ and $D(^2S)$ should follow (pseudo-) first-order kinetics unless there are secondary reactions which can deplete or reform these atomic species. Under first-order conditions, the temporal profile is given by

$$[X]_t = [X]_0 \exp[-(k_d + k[RH])t] = [X]_0 \exp[-k't]$$

where X is either $H(^2S)$ or $D(^2S)$, [RH] is either $[C_6H_6]$ or $[C_6D_6]$, k is the bimolecular rate constant for the reaction

$$X + RH \xrightarrow{k} products$$
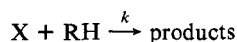
and k_d is the (first-order) decay rate of X in the absence of RH due to either reaction with impurities or diffusion from the reaction zone. A plot of ln $[X]_t$ vs. t, then, yields a straight line whose slope is $k' = k_d + k[RH]$. One such plot is shown in Figure 2 (curve A).
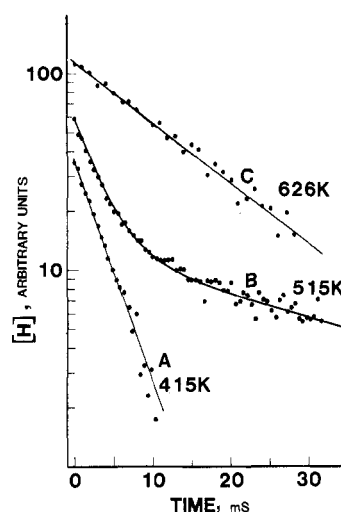

Figure 2. Semilog plot of H atom concentration vs. reaction time. Curve A: 415 K, $[C_6H_6] = 5.66 \times 10^{14}$ cm^3, $k' = 247$ s^{-1}. Curve B: 515 K, $[C_6H_6] = 1.95 \times 10^{14}$ cm^3, the solid line is best fit to the data of eq III (see text). Curve C: 626 K, $[C_6H_6] = 2.34 \times 10^{15}$, $k' = 80$ s^{-1}; note that the slope of H atom decay in the absence of $[C_6H_6]$ is also 80 s^{-1}. For visual clarity, curves A–C are vertically displaced, and the signal levels shown on the y axis do not reflect the actual signal levels.

In experiments aimed at measuring rate coefficients, the temporal profiles of $H(^2S)$ and $D(^2S)$ at fixed concentrations of C_6H_6 or C_6D_6 were obtained by averaging a suitable number of individual traces (20–1000). The decays were followed for at least two and in most cases three $1/e$ times. The k' value was determined from the plot of ln I vs. t, where I is the resonance fluorescence intensity which is directly proportional to the concentration of X. To obtain each value of k, the bimolecular rate coefficient, k' values were measured at a minimum of five and on the average six aromatic hydrocarbon concentrations. The plot of k' vs. [RH] was linear and the slope yielded the bimolecular rate constant.

The rate coefficients k_1-k_4 were measured by using the above procedure at temperatures ranging from 298 to 1000 K and are shown in Table I as well as in Figure 3. The errors quoted in the table include not only the error in the analysis of k' vs. [RH] data but also an 8% systematic error to account for the error in C_6H_6 concentration measurements. The values k_1-k_4 shown in Table I and Figure 3 were all derived from well-behaved systems. As will be pointed out below, there were temperature ranges where the system was ill-behaved and no rate coefficient data were measured under such conditions. The reported rate coefficients were not affected by secondary reactions as shown by many checks that were carried out. These checks included the variation of the initial concentrations of $H(^2S)$ and $D(^2S)$ by changing the photolysis flux and/or the concentration of the photolyte (in many cases the reactant itself). The photolysis flash was filtered by O_2 to eliminate vacuum UV radiation and the resultant k values were unaffected, thereby showing that the products of the UV photolysis of the aromatic hydrocarbon were not affecting the measured rate coefficient. At 298 and 470 K, the pressure in the system was varied from 10 to 100 torr with no measurable effect. The linear flow rate of gases through the reactor also did not have any effect.

In the case of reactions 1 and 4, the system was well-behaved until a temperature of 500 K. At temperatures between 500 and 560 K, the temporal profiles of $H(^2S)$ and $D(^2S)$ were not exponential. The decay rate was initially fast but decreased at longer reaction times. One such plot of H atom decay is shown in Figure 2 (curve B). As the temperature was increased, the initial faster part became faster and the slower decay moved to shorter times until 600 K, where we could not observe the faster decay at all. At still higher temperatures there was no observable enhancement in H atom decay rate due to reaction over that due to diffusion and impurity reactions. One such curve (which is essentially the same as the decay in the absence of C_6H_6) is shown in Figure 2

TABLE I: Absolute Rate Coefficients As a Function of Temperature for Reactions of H + C$_6$H$_6$ (k_1), H + C$_6$D$_6$ (k_2), D + C$_6$H$_6$ (k_3), and D + C$_6$D$_6$ (k_4)

temp, K	Ar press., torr	$10^{14}k_1{}^a$	$10^{14}k_2{}^a$	$10^{14}k_3{}^a$	$10^{14}k_4{}^a$
298	100	5.59 ± 0.80	4.80 ± 0.48		
298	30	4.99 ± 0.58			
298	12	5.57 ± 1.1			
346	100	12.2 ± 1.4			
379	100	22.8 ± 2.2	23.0 ± 2.5	20.8 ± 3.5	14.9 ± 1.7
379	25	24.2 ± 4.4			
412	100		44.9 ± 4.3		
415	100	34.6 ± 3.0			
458	100	60.3 ± 7.4			
465	100	63.3 ± 6.2	65.9 ± 6.1		50.5 ± 5.7
470	100	62.7 ± 6.3			
470	10	60.3 ± 6.5			
515	100	9.30 ± 1.09^b			
525	100	9.24 ± 1.33^b			
529	100	8.34 ± 2.53^b			
537	100	8.02 ± 1.11^b	1.25 ± 10^b		
545	100	8.01 ± 0.82^b			
550	100	4.91 ± 0.86^b			
555	100	6.34 ± 0.95^b			
570	100	6.29 ± 0.79^b			
612	100		55.7 ± 5.8		
633	100			184 ± 2.4	
684	100		81.2 ± 10.4		
710	100		108 ± 13		
788	100			403 ± 35	
832	100		233 ± 31		

^{a} Units: cm^3 molecule^{-1} s^{-1}. The errors include not only the 2σ precisions in fitting k' vs. [RH] to a straight line but also an 8% estimated systematic error in the knowledge of the RH concentration. ^{b} Curved pseudo-first-order decays; k_b calculated from initial slopes.
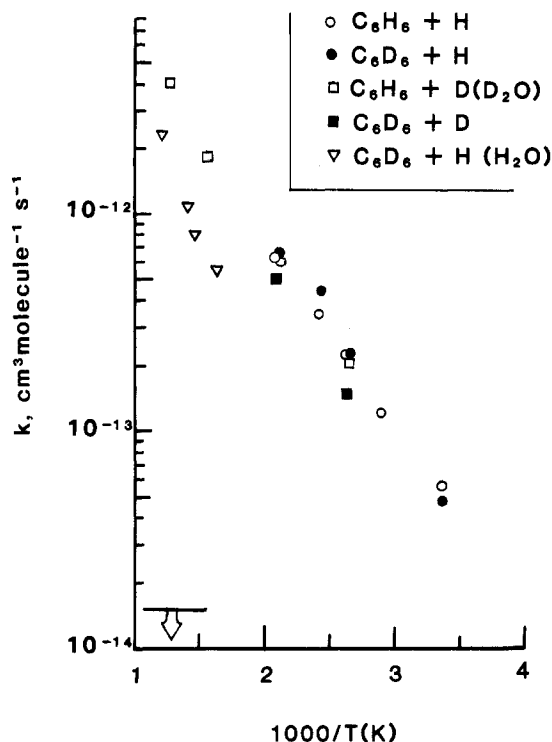

Figure 3. Arrhenius plots of k_1–k_4. The various symbols are shown in the legend. Whenever only D$_2$O or H$_2$O was used as the photolytic precursor of D or H atoms, they are shown in the legend. The line at the bottom left corner is a representation of the upper limit for the phenomenological rates coefficients k_1 and k_4 in that temperature range.

as curve C. These slow decays enabled us to place an upper limit of 1.5 × 10^{-14} cm^3 molecule^{-1} s^{-1} for the phenomenological rate coefficients for reactions 1 and 4 in the temperature range of 600–1000 K. The upper limit is shown as a line at the bottom of Figure 3.

Unlike reactions 1 and 4, reactions 2 and 3 were well-behaved as long as H$_2$O and D$_2$O were used as the photolytic precursors

of the atoms at $T > 500$ K. As shown in Figure 3, the value of k_2 keeps increasing with increases in temperature as does k_3 but with a slightly different value. In contrast to this behavior, if C$_6$H$_6$ and C$_6$D$_6$ were used as the source of H and D atoms, respectively, reactions 2 and 3 were ill-behaved as shown by curved decays, slower rate coefficients, and large dependencies on flash intensity, and, more important, the concentration of the photolytic precursor.
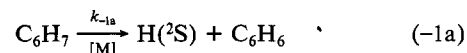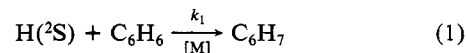
At temperatures less than 500 K, where all four reactions were well-behaved, k_1–k_4 were within experimental error indistinguishable from each other. The temperature dependencies of k_1 and k_2 have been calculated by using a linear least-squares analysis of the ln k vs. 1/T data and are as follows:
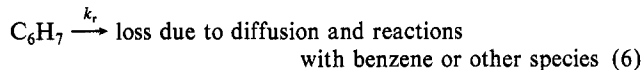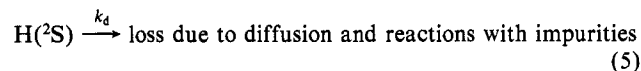
$$k_1 = (6.7 \pm 2.1) \times 10^{-11} \exp[-(2.17 \pm 0.13) \times 10^3/T] \quad (I)$$

$$k_2 = (8.7 \pm 6.6) \times 10^{-11} \exp[-(2.33 \pm 0.28) \times 10^3/T] \text{ cm}^3 \text{ molecule}^{-1} \text{ s}^{-1} \quad (II)$$

All errors are 2σ and $\sigma_A = A\sigma_{\ln A}$.

Decomposition of the Adduct. As mentioned in the previous section, we observed nonexponential H atom temporal profiles in the temperature range of 515–570 K for reaction 1. The decays became slower with increasing time, indicating the re-formation of H atoms at longer times. The initial parts of the decays were exponential for periods which decreased rapidly with increasing temperature such that at 580 K, the decay was not exponential for even 1 ms. The abrupt appearance (on a temperature scale) of this behavior indicates that a very high activation energy process is responsible for the H atom regeneration. It was indicated in the Introduction section that the reaction of H atoms with benzene proceeds via an addition pathway leading to the formation of cyclohexadienyl radical. In the following section we will first assume the cyclohexadienyl radical to be the source of H atom re-formation and at the end of the section we will justify this assumption. The reactions that can take place in the H + C$_6$H$_6$ reaction system are

$$H(^2S) + C_6H_6 \xrightarrow[\text{[M]}]{k_1} C_6H_7 \quad (1)$$

$$C_6H_7 \xrightarrow[\text{[M]}]{k_{-1a}} H(^2S) + C_6H_6 \quad (-1a)$$

$H(^2S) \xrightarrow{k_d}$ loss due to diffusion and reactions with impurities

$$(5)$$

$C_6H_7 \xrightarrow{k_r}$ loss due to diffusion and reactions

with benzene or other species (6)

The abstraction of ring hydrogen atom is negligible, as will be shown in the Discussion section.

Both reactions 1 and −1a can be pressure dependent. Therefore, the value of rate coefficient k_1 needed to calculate k_{-1a} (and later the equilibrium constant) should be that which is applicable under the temperature and pressure conditions where k_{-1a} was derived. At 470 K it was shown that a 10-fold change in pressure had no effect on the measured value of k_1 (see Table I). Therefore, it is unlikely that reaction 1 is very far from its high-pressure second-order limit in the temperature range of 515–570 K where k_{-1a} was evaluated. Moreover, in experiments up to 540 K, k_1 was directly measured and found to be, within experimental error, that obtained from an extrapolation of the low-temperature data. Lastly, as shown by reaction 2, $\ln k_2$ varies linearly with $1/T$ even up to 832 K. Therefore, we are confident that the value of k_1 used in these calculations is quite accurate.

The differential equation governing the time dependence of $[H(^2S)]$ in the above reaction scheme has an analytical solution given by eq III.

$$[H(^2S)]_t = ([H(^2S)]_0/Z)\{R \exp(\lambda_1 t) - S \exp(\lambda_2 t)\} \qquad (III)$$

where

$$R = k_{-1a} + k_r + \lambda_1$$

$$S = k_{-1a} + k_r + \lambda_2$$

$$\lambda_1 = 0.5(Z - X)$$

$$\lambda_2 = -0.5(Z + X)$$

$$Z = (X^2 - 4Y)^{1/2}$$

$$X = k_1[C_6H_6] + k_{-1a} + k_d + k_r$$

$$Y = k_{-1a}k_d + k_dk_r + k_1[C_6H_6]k_r$$

The nonexponential decays that were observed at temperatures between 515 and 569 K in the case of H + C_6H_6 reaction were fitted to expression III by varying k_{-1a} and k_r. One such fit is shown in Figure 2 (curve B) as the solid line. To carry out these fits the value of k_1 at the given temperature is needed. It was obtained by two methods: (1) the low-temperature ($T < 500$ K) data were extrapolated, by assuming the validity of the Arrhenius expression, to the experimental temperature; (2) the fast exponential components of the decays such as the one shown in Figure 2 (curve B) were attributed to the forward reaction (i.e., reaction 1 + reaction 5 only and k_1 was extracted from the calculated slopes. The second method was useful only up to 540 K. At higher temperatures the H atom decays became nonexponential at very short reaction times and hence k_1 values could not be extracted from these curves. At these higher temperatures, only the first method was used to evaluate k_1. The nonexponential H atom temporal profiles were recorded at seven temperatures in the range 515–569 K where well-defined curves were seen. At each temperature k_d, the first-order decay rate of H atoms in the absence of C_6H_6, was measured by photolyzing H_2O. H atom temporal profiles were acquired at a minimum of three and an average of four benzene concentrations. The benzene concentration was varied by at least a factor of 4. Since the long reaction time data (i.e., the data at times when [H] has decayed by more than $1/e$ time for reaction 1 was the crucial component for the determination of k_{-1a}, a very large number of traces were averaged to obtain good definition of [H] at long times. One of the crucial parameters in the curve-fitting procedure is t_0, the time at which H atoms are photolytically created. Since our photoflash lasts for ∼50 µs and since, when averaging multiple pulses, the signal averager generates an uncertainty of 100 µs (when the dwell time
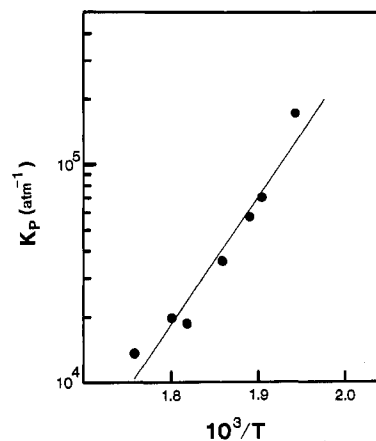

Figure 4. Plot of ln K_p (the equilibrium constant for reaction 1 ⇌ reaction −1) as a function of $1/T$. The solid line is the weighted linear least-squares fit of the data. Note that the datum at the highest temperature had a large error associated with it.

is 1 ms), the uncertainty in t_0 was 200 µs. This uncertainty did not introduce a significant error in the calculated values of k_{-1a}. Except at the highest temperature, the precision of the measured values of k_{-1} was quite good and on the average it was ∼15%. It was also observed that k_r was small, 50 s⁻¹, and independent of benzene concentration. The obtained values of k_{-1a} ranged from 77 s⁻¹ at 515 K to 1400 s⁻¹ at 569 K. A linear least-squares analysis of the ln k_{-1a} vs. $1/T$ data yields the expression

$$k_{-1a} = (1.3^{+4.8}_{-1.3}) \times 10^{16} \exp\{-(1.67 \pm 0.39) \times 10^4/T\} \text{ s}^{-1} \quad (IV)$$

Even though it is possible to calculate the heat of reaction −1a by using the activation energies for reactions 1 and −1a, the cumulative error in the value of ΔH_f (reaction) will be very large. A less erroneous method involves calculating the equilibrium constant, $K = k_1/k_{-1a}$, at the seven temperatures studied here, and extracting the ΔH_f^{298} value by using the calculated free energy change[13]

$$-RT \ln K_p = \Delta G_R = \Delta H_R - T\Delta S_R \qquad (V)$$

where K_p is the equilibrium constant in pressure units and ΔG_R, ΔH_R, and ΔS_R are the free energy, enthalpy, and entropy changes in reaction. Again ΔS_R could be calculated to obtain ΔH_R. On the other hand

$$\ln K_p = -\Delta H_R/RT + \Delta S_R/R \qquad (VI)$$

A plot of ln K_p vs. $1/T$ yields a straight line as shown in Figure 4 with a slope of $-\Delta H_R/R$. A linear least-squares fit of our data, weighted according to the number of experiments and precision of the measured value of k_r, yields $\Delta H_R^{542} = 26.7$ kcal/mol. ΔH_R^{298} was calculated (using an estimated value of C_p for C_6H_7) to be 26.2 kcal/mol. Using this value we obtain 45.7 ± 2.8 kcal/mol for $\Delta H_f^{298}(C_6H_7)$. The quoted error is 2σ and is a measure of precision only.

In the above description and calculations a few assumptions have been made. First, it has been assumed that C_6H_7 formed in reaction 1 is completely thermalized before it decomposes. This is a justifiable assumption since the decomposition takes place on millisecond time scales. The complex formed in reaction 1 will undergo thousands of collisions with the bath gas prior to decomposition. Hence, it is almost assured that the complex is thermalized before decomposition. Second, it is assumed that the k_1 value used is applicable under these conditions (see earlier justification). Lastly, it is assumed that H atom formation is due to the decomposition of C_6H_7. It was observed that the H atom decays became nonexponential at longer reaction times while they are exponential immediately following the photolysis pulse. At higher benzene concentrations, the decays were exponential for

(13) S. W. Benson, "Thermochemical Kinetics", Wiley, New York, 1968.

TABLE II: Summary of Rate Constants Data for Reaction 1

exptl method	$10^{14}k_1(298\ K)$, cm^3 molecule^{-1} s^{-1}	A, cm^3 molecule^{-1} s^{-1}	E/R, deg^{-1}	temp range, K	ref
a	3.21	2.12×10^{-11}	1950 ± 300	326–476	5
	$(4.3)^f$	$(4.28 \times 10^{-12})^f$	$(1370 \pm 310)^f$		
b	9.5	1.00×10^{-11}	1360 ± 100	g	8
b	3.0				9
b, c	2.2	1.15×10^{-11}	1870 ± 350	296–473	10
d	6.15	1.3×10^{-11}	1670	298–362	6
d	5.9	9.8×10^{-11}	2170	298–383	7
e	5.59	7.4×10^{-11}	2170 ± 130	298–470	this work

^{a}CW γ-radiolysis. k_1 measured relative to H + C$_3$H$_8$ reaction rate coefficient. ^{b}Discharge flow tube equipped with mass spectrometer detection. ^{c}Discharge flow tube equipped with ESR detection. ^{d}e-beam pulse radiolysis in association with UV absorption. ^{e}Pulsed photolysis–resonance fluorescence. ^{f}Calculated on the basis of the recently recommended[16] value of 1.66×10^{-11} exp($-3130/T$) for H + C$_3$H$_8$ reaction rate coefficient. ^{g}Not specified in their paper but is deduced to be between 298 and 398 K.

a larger decrease in [H] than at lower benzene concentrations. This observation indicates that the time constant for the H atom re-reformation process is independent of benzene concentration, which is borne out by the invariance of k_{-1a} to changes in [C$_6$H$_6$]. Addition of a small amount of O$_2$ at 540 K made the H atom temporal profile exponential, thereby indicating that the species that leads to H atom regeneration reacts with O$_2$ (a typical behavior for a free radical) and thereby avoids decomposition. The calculated value of k_{-1a} was also independent of [H]$_0$. In the next section it will be shown that H atoms are formed in the reaction of D with C$_6$H$_6$. These arguments together clearly show that the H atom regeneration is due to the decomposition of the adduct and the adduct is cyclohexadienyl radical as was indicated earlier.

A few experiments at 525, 555, and 570 K were carried out on the D + C$_6$D$_6$ system in a manner analogous to the one described above for the H + C$_6$H$_6$ system. It was observed that at a given temperature, the decomposition of the C$_6$D$_7$ adduct was slower than in the case of C$_6$H$_7$. Since this system was studied merely to confirm the decomposition of the adduct in the case of the D + C$_6$D$_6$ system and not studied extensively, we have not carried out the calculation of the heat of formation C$_6$D$_7$ adduct.

In summary, it has been calculated that the heat of formation of the adduct in reaction 1, the cyclohexadienyl radical, is 45.7 kcal/mol and that expression IV gives the rate of its thermal decomposition.

Yield of H Atoms in Reaction 3. In order to check for the isotope exchange in reaction 3 reported previously by two groups[8,9] and to verify the reaction mechanism used in the previous section in deriving the kinetic and thermodynamic quantities, reaction 3 was extensively studied at 630 K. The basic idea behind the experiments carried out at this temperature is to create a known concentration of D atoms in excess C$_6$H$_6$ and then monitor H atoms as a function of time. This experiment is made possible by two factors: (1) H atoms apparently do not undergo a net reaction with C$_6$H$_6$ at this temperature (2) H atoms can be detected, with complete selectivity, in the presence of D atoms. When D atoms are generated by photolysis of D$_2$O in the presence of C$_6$H$_6$, H atoms are indeed produced. To place the amount of H atoms produced in reaction 3 and the initial D atoms produced by photolysis on the same concentration scale, it is necessary to know the absolute concentrations of D and H atoms produced, know the relative detection sensitivities for D and H atoms, or be able to quantitatively convert D atoms into H, in which case only the relative H atom signal levels need to be measured. We adopted the third method since it is least prone to errors in experimental setups such as ours. The experiments were carried out in three steps listed below. (a) A known concentration of C$_6$H$_6$ in 100 torr of Ar buffer gas was photolyzed at a fixed photolysis energy. The H atom signal S_1 and the decay rate of H atoms were measured. As mentioned earlier, H atoms do not undergo a net reaction with C$_6$H$_6$ at 630 K and therefore disappear with a time constant characterized by k_d. (b) A mixture containing the same concentration of C$_6$H$_6$ as above and a known concentration of D$_2$O in 100 torr of Ar was photolyzed at the same photolysis energy as in step 1. In this case, in addition to the H

atoms produced synchronous with the photolysis pulse, there is an additional time-dependent H atom signal which increases, reaches a maximum, and then decays with a time constant k_d. (c) A mixture of D$_2$O (same concentration as step b and 200–650 mtorr at H$_2$ in 100 torr of Ar is photolyzed at the same energy as in steps a and b. In this experiment, H atoms are produced by the following reaction sequence:

$$D_2O \xrightarrow{h\nu} OD + D \tag{7}$$

$$OD + H_2 \xrightarrow{k_8} HDO + H \tag{8}$$

$$D + H_2 \xrightarrow{k_9} HD + H \tag{9}$$
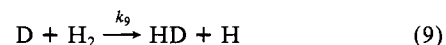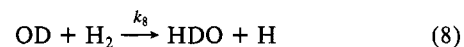
It is necessary to note that for each D atom formed in step b there are two H atoms produced in step c. (The rate coefficients for reactions 8 and 9 are known[14] and with the amount of H$_2$ used, the reactions 8 and 9 go to completion in less than a few microseconds.)

In step b, the H atoms are not only being generated by reaction 3 but also being depleted due to diffusion. Therefore, the maximum signal seen in step b is not a true indication of the amount of H atoms produced. To calculate the concentration of H atoms that would have been produced when reaction 3 went to completion in the absence of any H atom loss processes, we used the method described in one of our earlier papers.[15] When this correction is made, which accounted for an increase of 10%, the signal obtained is S_2; S_2 is a measure of the sum of H atoms produced by C$_6$H$_6$ photolysis and via reaction 3. Half the signal produced in step c, S_3, is proportional to the amount of D atoms produced in step b. Therefore, the yield of H atoms in reaction 3 is given by $(S_2 - S_1)/(0.5S_3)$. It is important to point out that S_1, S_2, and S_3 have been normalized to take into account absorption of Lyman-α by D$_2$O and C$_6$H$_6$.

Twelve separate sets of experiments were carried out with variations in [C$_6$H$_6$], [H$_2$], [D$_2$] and the photolysis flux. The yield determined from these 12 experiments was 1.01 ± 0.20 where the error is 1σ. The measured yield was not affected by the variation of the above-mentioned parameters, thereby indicating the absence of secondary reaction contributions. OD formed in D$_2$O photolysis does not produce H atoms via reaction with C$_6$H$_6$ as shown by the absence of a time-dependent H atom signal when a mixture of H$_2$O and C$_6$H$_6$ is photolyzed at 630 K. (Since we know the rate coefficient for the reaction of OH with C$_6$H$_6$,[1] we can predict the fastest possible rate for H production.) The error in our measurement is such that we cannot rule out a small fraction of the adduct decomposing back to give D atoms.

(14) Even though OD + H$_2$ has not been directly determined, it should be very close to OH + H$_2$, which has been well studied; see A. R. Ravishankara, J. M. Nicovich, R. L. Thompson, and F. P. Tully, *J. Phys. Chem.*, **85**, 2498 (1981). For D + H$_2$ rate coefficients see H. S. Johnston, "Gas Phase Reaction Rate Theory", Ronald Press, New York, 1967.

(15) P. H. Wine and A. R. Ravishankara, *Chem. Phys. Lett.*, **77**, 103 (1981).

To summarize, we see the formation of H atoms in reaction 3 and for each D atom consumed approximately one H atom is formed.
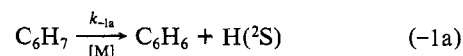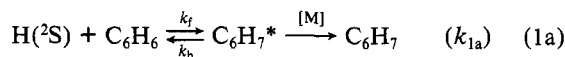
Discussion

The reaction between H(^{2}S) and C_6H_6 has been investigated by many groups at low temperatures, i.e., $T < 500$ K. Table II lists k_1(298 K), the activation energy E_1, and the preexponential factor A for reaction 1 measured (and in some cases deduced) by various investigators. It is clear from Table II that the reported values are in very poor agreement. Yang[5] measured the value between 326 and 476 K by a competitive method where H atoms were produced by γ-radiolysis. Extrapolation of his results to 298 K yields k_1(298 K) = 3.2 × 10^{-14} cm^3 molecule^{-1} s^{-1}. When a more recent recommendation for the rate coefficient for the H + C_3H_8 reaction[16] (the reaction relative to which reaction 1 was studied) is used, his k_1(298 K) is in better agreement with the present measurement. However, the Arrhenius parameters would be in worse agreement as shown in Table I. The technique used by Allen et al.,[17] i.e., removal of H atom by molybdenum oxide as a measure of H atom concentration, has been questioned and is likely to be wrong. Of the four "direct studies", the work of Sauer and co-workers[6,7] was carried out by monitoring the growth of a transient (cyclohexadienyl radical) UV absorption under pseudo-first-order conditions in H atoms (i.e., $[C_6H_6] \gg$ [H]). The values obtained by Sauer and co-workers[6,7] are in excellent agreement with our results. The other three studies were carried out in discharge flow tubes. Kim et al.[8] studied reactions 1 and 2 under pseudo-first-order conditions. They did not study reaction 1 under conditions of $[C_6H_6] \gg$ [H] since they were concerned about the regeneration of H atoms. Under the conditions of [H] $\gg [C_6H_6]$ they measured k_1(298 K) to be 9.45 × 10^{-14} cm^3 molecule^{-1} s^{-1}. This value is 50% higher than that measured by us. Knutti and Buhler[9] used a method very similar to Kim et al.[8] but obtained a value of (3.0 ± 0.3) × 10^{-14} cm^3 molecule^{-1} s^{-1} under the conditions $[C_6H_6] \gg$ [H]. The values of k_1 measured by Hoyermann et al.[10] are lower than our values even though their activation energy is similar to ours. In their experiments, these workers estimated a stoichiometry factor which was greater than 5 (i.e., for each H atom that reacts with C_6H_6, nearly five other H atoms are lost due to secondary reactions). A possible reason for the discrepancy between the two studies is the inaccuracy of the stoichiometry factors. It is impractical to discuss at great lengths the reasons for the discrepancies between our results and the values of these three low-pressure studies. However, at least in hindsight, it is quite clear that a discharge flow experiment under conditions of very high radical concentrations is ill-suited for measurement of elementary reaction rate coefficients for an addition reaction which is quite slow. The sticking of reactants (both radicals and stable molecules) to the walls, and the consequent enhanced wall loss processes, the occurrence of secondary reactions which can regenerate reactants, and the condition of low bath gas pressures relative to the atom concentrations can all lead to large errors in the measured rate coefficient. In addition, even when studies are carried out with the stable reactant in excess over the free radical, the ratio of the molecule to free radical should be kept very high in the case of slow reaction to avoid secondary reactions.

We have carried out measurements of k_1–k_4 under pseudo-first-order conditions with the concentration of benzenes several orders of magnitude greater than the H or D atom concentration. Furthermore, we carried out extensive tests to check for secondary reactions and convinced ourselves of the absence of such contributions. Therefore, we believe that the measurements presented

in this paper are devoid of any major errors.

One of the difficulties in carrying out the measurements of k_1–k_4 at lower temperatures, i.e., $T < 400$ K, is that benzene absorbs Lyman-α radiation. Since the rate coefficients are quite small, large concentrations of benzenes have to be added to the reactor to obtain pseudo-first-order decay rates (k') which are much higher than k_d. At these high concentrations of benzenes, the resonance fluorescence signals are attenuated by a large amount. Therefore, only reactions 1 and 2 were studied at 298 K. In the case of reaction 3, a few measurements were carried out at 298 K and the measured value was approximately the same as k_1 and k_2.

The possible mechanisms for the reaction of H or D atoms with C_6H_6 or C_6D_6 were presented in the Introduction section and are repeated for the case of reaction 1. The measured value of k_1

$$H(^2S) + C_6H_6 \underset{k_b}{\overset{k_f}{\rightleftharpoons}} C_6H_7^* \xrightarrow{\text{[M]}} C_6H_7 \qquad (k_{1a}) \qquad (1a)$$

$$C_6H_7 \xrightarrow{\text{[M]}} C_6H_6 + H(^2S) \qquad\qquad (-1a)$$

$$H(^2S) + C_6H_6 \xrightarrow{k_{1b}} C_6H_5 + H_2 \qquad\qquad (1b)$$

is the sum of $k_{1a} + k_{1b}$. At high temperatures, i.e., $T > 600$ K, the reverse reaction rate coefficient k_{-1a} becomes very large. Therefore, the addition channel is essentially unobserved for reaction 1. The rate coefficients that we determined at 700–900 K are only upper limits. Therefore, k_{1b} could at most be as large as the upper limit, i.e., 1.5 × 10^{-14} cm^3 molecule^{-1} s^{-1} at 700–900 K. Assuming the endothermicity of reaction 1b to be the activation energy for this reaction in conjunction with the measured upper limit, at 700 K we can calculate

$$k_{1b} \sim 5 \times 10^{-12} \exp(-8100/RT) \text{ cm}^3 \text{ molecule}^{-1} \text{ s}^{-1}$$

This expression clearly shows the negligible contribution of reaction 1b at any temperature less than 1000 K. Therefore, we can completely ignore the ring hydrogen abstraction at lower temperatures.

Now turning to reaction 1a, we measured k_1 at three diluent gas pressures (12, 30, and 100 torr) at 298 K. The measured values were independent of pressure, within the combined experimental errors. Therefore, it is clear that k_1 is in the high-pressure second-order limit even at 12 torr. The agreement between our value and that obtained by Sauer and Ward is a further confirmation of the high-pressure limit being as low as 12 torr. It is not surprising that the high-pressure limit for reaction 1 is reached at a few torr considering the complexity of C_6H_6, and the consequent availability of a large number of internal modes for the distribution of the energy released in the addition process. It is inappropriate to compare the results of Sauer and Ward and the present study with the flow tube results in a search for the pressure-dependent region of k_1 since in the latter experiments the major quencher of the adduct was the wall of the reactor and hence the overall reaction was not truly homogeneous.

Even though reaction 1 proceeds through an addition pathway, it exhibits a positive activation energy. In the case of the OH + C_6H_6 reaction there is no measurable temperature dependence for the high-pressure limiting rate coefficient.[1] On the other hand, O(^{3}P) also undergoes an addition reaction with C_6H_6 and exhibits a large positive activation energy.[3] Therefore, even though the origin of the barrier for the reaction is not clear, its presence is not very surprising.

We do not observe any kinetic isotope effect, i.e., $k_1/k_2 = 1$. This is in contrast to the observations of Kim et al.[8] and Knutti and Buhler,[9] who measured $k_1/k_2 \sim 0.5$. Kim et al. attributed the observed kinetic isotope effect mainly to the subsequent chemistry of C_6H_7. Knutti and Buhler agree with this interpretation. However, they still ascribed their measured value of the rate coefficient to the elementary reaction 1. This assertion is not only inconsistent with their own results but also not very understandable. An addition reaction such as reaction 1 is not expected to exhibit a kinetic isotope effect as large as 0.5. The

(16) F. Westley, "Table of Recommended Rate Constants for Chemical Reactions Occurring in Combustion", Vol. NBSIR-79-1941, National Bureau of Standards, Washington, DC, 1979.

(17) P. E. Allen, H. W. Melville, and J. C. Robb, *Proc. R. Soc. London, Ser. A*, **218**, 311 (1953).

(18) D. F. McMillen and D. M. Golden, *Am. Rev. Phys. Chem.*, **33**, 493 (1982).

lack of kinetic isotope effect seen by us is certainly consistent with the above mechanism.

The explanation for the observation of measurable rates in the cases of reactions 2 and 3 is quite obvious from the above reaction mechanism. The cyclohexadienyl radical formed in the case of, say, reaction 2 is C_6D_6H. This radical can decompose by two channels:

$$C_6D_6 \xrightarrow{k_{-2a}} C_6D_6 + H \qquad (-2a)$$

$$\xrightarrow{k_{-2b}} C_6D_5H + D \qquad (-2b)$$

It is expected, as argued earlier, that the cyclohexadienyl radical is thermalized. Therefore, it is quite likely that this thermalized adduct can scramble H atoms and therefore, statistically speaking, reaction $-2b$ would be 6 times more prevalent than reaction $-2a$. Since only H atom disappearance is monitored and since any subsequent reactions of the product D atom with C_6D_6 would lead only to D atoms, the rate coefficient measured would be very close to that for reaction 2. This indeed is the case as shown by the values of k_2 and k_3 at high temperatures, i.e., $T > 600$ K. They are very close to the values obtained from linear extrapolation of the low-temperature Arrhenius plots. This explanation is completely consistent with the unit yield of H in reaction 3. A similar argument has been proposed by Benson and Shaw[10] to explain the isotope exchange seen by them in their experiments on the thermal decomposition of cyclohexadiene in the presence of benzene-d_6.

The value of k_2 is lower than that of k_3 at $T > 700$ K. One possible explanation for this observation may lie in the fact that as the decomposition rate of the adduct gets very large, the adduct might not have sufficient time to thermalize. However, an extrapolation of our thermal decomposition data suggests that even at 900 K the adduct must undergo tens of collisions before decomposition. The second possible explanation is that process-2

exhibits a large kinetic isotope effect; i.e., k_{-2a}/k_{-2b} is large. A check for such a process would involve measuring the rate coefficient for reaction 2 on very short time scales where reaction -2 would not regenerate H atoms. Such short time scale experiments are not feasible because of the lack of a suitable H atom laser photolytic source which would not react with D and be thermally stable at these high temperatures. The use of a short pulsed laser with a pulse width <1 μs would be essential since light output of our flash lamp lasts for ca. 50 μs and hence experiments cannot be carried out on microsecond time scales.

The heat of formation of the cyclohexadienyl radical that we measured using the equilibrium constants is 45.7 kcal/mol. The value is slightly lower than the 47 kcal/mol reported by McMillen and Golden,[18] which was based on prior estimations, but should be considered in excellent agreement within the precision of our measurement. This procedure for the heat of formation determination was based on measurements over a very small temperature range and yet, as seen here, yields a very good value.

To summarize, we have carried out measurements of the rate coefficients for reactions 1–4 and shown addition of H/D atoms to the benzene ring to be the predominant reaction pathway. We have also measured the rate of thermal decomposition of the adduct and deduced the heat of formation of this adduct, i.e., cyclohexadienyl free radical. Lastly, it is necessary to point out that even though the cyclohexadienyl radical decomposes at high temperatures, depending on its reactivity with other species, reaction 1 could be important in combustion processes.

Registry No. C_6H_6, 71-43-2; C_6D_6, 1076-43-3; H, 12385-13-6; D, 16873-17-9; C_6H_7, 12169-67-4.

Solvent Effect on the Kinetics of Complexation of Alkali Ions with the Macrocyclic Ligand 18-Crown-6

Cindy Chen,[†] **William Wallace,**[†] **Edward Eyring,**[‡] **and Sergio Petrucci***[†]

Departments of Chemistry, Polytechnic Institute of New York, Farmingdale, New York 11735, and University of Utah, Salt Lake City, Utah 84112 (Received: July 18, 1983)

The kinetics of complexation of alkali ions with the macrocycle 18C6 in the solvents dimethylformamide and ethanol have been studied by pulse and resonation ultrasonic relaxation techniques. The latter is illustrated in detail. The Eigen–Winkler mechanism is capable of interpreting the data. For NaSCN + 18C6 in DMF at high concentration, however, an unaccounted complication occurs. Also, it has been found that the nature of the solvent may affect the number of observable steps seen during the complexation process. This influence does not appear to be due to the permittivity of the solvent but rather to its donor or solvating ability toward the cation.

Introduction

Current ideas of short-range interactions in electrolyte solutions envisage the solvent and the anions (or other ligands present) as being competitors for the first-coordination sphere of the cations. Biological relevance (exemplified by model studies of processes occurring in human cells) has pushed the study of coordination of macrocyclic ligands to the forefront of present interests in electrolyte solutions.[1] Here the study is complicated by the presence of three potential ligands (the solvent, the anion, and

the macrocycle) and by the multidentate nature of the macrocycle.

In previous work of more exploratory nature, we studied the kinetics of complexation of alkali-metal ions with crown ethers in dimethylformamide (DMF)[2] and methanol.[3] In the former solvent only the faster relaxation could be studied with the ultrasonic technique available to use at that time. In the present

(1) G. A. Melson, Ed., "Coordination Chemistry of Macrocyclic Compounds", Plenum Press, New York, 1979; R. M. Izatt, Ed., "Progress in Macrocyclic Chemistry", Vol. II, Wiley, New York, 1981.
(2) K. Maynard, D. E. Irish, E. M. Eyring, and S. Petrucci, *J. Phys. Chem.*, **88**, 729 (1984).
(3) C. Chen and S. Petrucci, *J. Phys. Chem.*, **86**, 2601 (1982).

[†] Department of Chemistry, Polytechnic Institute of New York.
[‡] Department of Chemistry, University of Utah.